Astron. Astrophys. 348, 815–824 (1999)

ASTRONOMY
AND
ASTROPHYSICS

Theoretical UBVI light curves of RR Lyrae stars

E.A. Dorfi and M.U. Feuchtinger

Institut für Astronomie der Universität Wien, Türkenschanzstrasse 17, A-1180 Wien, Austria

Received 2 February 1999 / Accepted 28 May 1999

Abstract. By performing detailed frequency-dependent radiative transfer computations we have obtained UBVI light curves of nonlinear RR Lyrae models, which recently have been calculated by the Vienna nonlinear convective pulsation code. For two sets of stellar parameters ($M = 0.65\,\mathrm{M}_\odot$, $L = 52.5\,\mathrm{L}_\odot$, $Z = 0.001$ as well as $M = 0.75\,\mathrm{M}_\odot$, $L = 52.5\,\mathrm{L}_\odot$, $Z = 0.0001$) the fundamental and the first overtone limit cycle solutions have been calculated for effective temperatures ranging from $6000\,\mathrm{K}$ to $7200\,\mathrm{K}$. The results of these computations are used as input for the radiative transfer calculations.

The properties of the UBVI light curves have been analyzed by means of standard Fourier decomposition and a detailed comparison to recent observations has been performed. As main results we find an good agreement with important observed RR Lyrae properties like pulsation amplitudes and Fourier parameters in B-, V-, and I-bands. Additionally from these synthetic colour light curves we derive linear transformation laws between amplitudes as well as Fourier parameters in the different passbands.

Key words: hydrodynamics – radiative transfer – stars: oscillations – stars: variables: RR Lyr

1. Introduction

During the past years a number of observational investigation (e.g. Udalski et al. 1994, Alcock et al. 1998, Walker 1998, Clement & Shelton 1997) considerably increased the available experimental data about RR Lyrae light curves. In parallel several theoretical investigations (e.g. Bono & Stellingwerf 1994, Bono et al. 1997, Feuchtinger & Dorfi 1998, Kolláth et al. 1998, Feuchtinger 1998, 1999ab) provide detailed nonlinear models of these stars, and a comparison of theoretical and observed light curves is crucial for providing new insight into the involved physical mechanisms governing pulsating stars.

While RR Lyrae light curves are observed in certain spectral bands (mostly B, V, R or I), theoretical pulsation calculations are mainly performed by adopting grey (i.e. frequency-integrated) opacities, yielding bolometric light curves. Consequently a detailed comparison lacks from this difference in spectral information (e.g. Kovács & Kanbur 1997). Depending on the particular passband employed, differences vary from few percents (eg. V-band, Feuchtinger 1999b) to considerable deviations (e.g. I-band, Morgan et al. 1998, subsequently MSB98).

A first approach to this problem is to use the photospheric values of temperature and effective gravity at each pulsation phase as input for static model atmospheres (Kurucz 1993). The resulting bolometric corrections can be applied to the theoretical light curves (Simon & Kanbur 1995, Kovács & Kanbur 1997, Bono et al. 1997).

In this paper we present a more accurate method of transforming bolometric light curves into the desired passband by computing a frequency-dependent radiative transfer on top of the nonlinear models. For each pulsation phase we obtain a theoretical spectrum, and the convolution of these synthetic spectra with the corresponding filter curves leads to synthetic colour light curves.

A powerfull tool for analyzing and comparing light curves of pulsating stars is provided by Fourier decomposition (Simon & Lee 1981). In the case of RR Lyrae stars an number of observational investigations provide Fourier fits of both RRab and RRc stars (see Sect. 3.3 for references). Unfortunally, these data are meassured in different photometric bands, and clearly the Fourier parameters of a particular light curve depend on the employed filter. Therefore even a comparison between different observational results can be difficult, if different passbands are used (MSB98).

By using the results of our frequency-dependent radiative transfer, detailed comparisons to observations can be performed for any desired passband. In Sect. 2 we give a brief summary of the physical input for both the radiative transfer calculations and the underlying nonlinear models. Sect. 3 discusses the basic features of the theoretical UBVI light curves in the light of recent observations and Sect. 4 closes the paper with some conclusions.

2. Theoretical RR Lyrae models

Based on recent nonlinear convective pulsation calculations (Feuchtinger 1999b) two sets of RR Lyrae models oscillating in the fundamental or the first overtone limit cycle have been

Send offprint requests to: E.A. Dorfi
(EAD@ASTRO.UNIVIE.AC.AT)

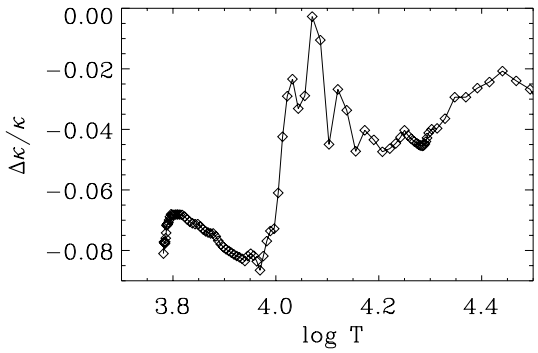

Fig. 1. The relative difference $\Delta\kappa/\kappa$ of the Rosseland means between the OPAL-Alexaner opacities and the Kurucz opacities in a RR Lyrae atmosphere from 6000 to 30000 K for a model with $M = 0.65\,\mathrm{M}_\odot$, $L = 52.5\,\mathrm{L}_\odot$, $T_{\rm eff} = 6600\,\mathrm{K}$, $Z = 0.001$.

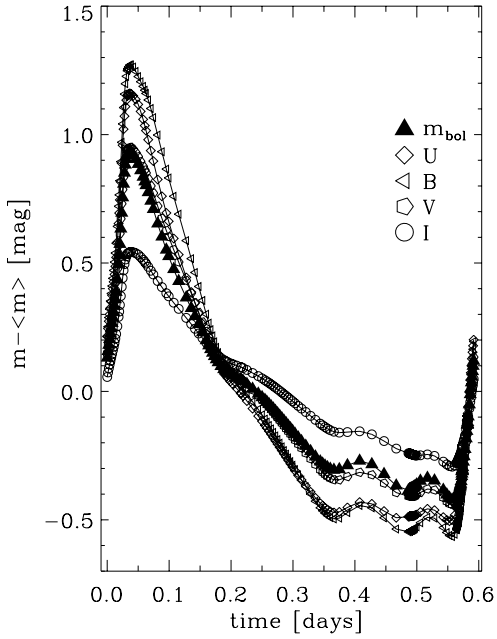

Fig. 2. Theoretical U-, B-, V-, I-band and bolometric light curves plotted around their mean values in each band for a fundamental mode pulsator with $M = 0.65\,\mathrm{M}_\odot$, $L = 52.5\,\mathrm{L}_\odot$, $T_{\rm eff} = 6600\,\mathrm{K}$, $Z = 0.001$.

used to perform detailed spherically symmetric and frequency dependent radiative transfer calculations on top of the grey radiation hydrodynamical models. Stellar parameters correspond to $M = 0.65\,\mathrm{M}_\odot$, $L = 52.5\,\mathrm{L}_\odot$, $Z = 0.001$ (sequence A) and $M = 0.75\,\mathrm{M}_\odot$, $L = 52.5\,\mathrm{L}_\odot$, $Z = 0.0001$ (sequence B) and effective temperatures range from 6000 K to 7200 K. The numerical techniques used for calculating nonlinear pulsation models have been discussed extensively in Dorfi & Feuchtinger (1995). The model of turbulent convection adopted in these computations is explained in Wuchterl & Feuchtinger (1998) and for further physical details we refer to Feuchtinger (1999ab).

The nonlinear models based on Rosseland mean opacities provide the temperature, density and pressure structure for the non-grey radiative transfer. The frequency grid comprises 1212 frequency points and opacities provided by Kurucz (1993) have been used. It is important to note that these frequency-dependent opacities differ from the opacities used for the underlying nonlinear pulsation models (OPAL opacities (Iglesias & Rogers 1991) augmented by the Alexander molecule opacities (Alexander et al. 1989) at the low temperature end, cf. Feuchtinger 1999b). Detailed tests involving the calculation of Rosseland mean opacities from the Kurucz opacities and their influence on the pulsational dynamics will be presented in a companion paper (Dorfi et al. 1999). However, as can be inferred from Fig. 1, differences between the OPAL-Alexander and the Kurucz Rosseland means throughout the outer part of a typical RR Lyrae envelope remain well below 10%. Therefore we do not expect major changes in the pulsational properties when using the Kurucz opacities for the nonlinear computations.

We solve the time-independent radiation transfer equation in spherical symmetry by integrating along characteristics (Yorke 1980, Balluch 1988) and adopt a Planck spectrum at the inner boundary located at $\tau = 100$ (τ denoting the grey optical depth). Typically about 100 radial grid points corresponding to the radiation hydrodynamical model are used and this number is augmented by 40 impact parameters resolving the central region within the radius defined through $\kappa_{\rm R,in}$. For calculating the source function S_ν we assume LTE throughout the whole region. A more detailed description including colour calibrations and theoretical bolometric corrections will be given in a forthcoming paper (Dorfi et al. 1999).

After having computed the theoretical spectra on the 1212 frequency points for each time-step of the nonlinear model, these data are convolved with the standard Johnson UBVRI filter curves (e.g. Landolt- Börnstein 1982) to obtain synthetic colours. For this purpose the filter curves have been interpolated at the frequency points by means of rational splines (Späth 1983). Taking a different representation of the UBVI filter curves (e.g. Bessell 1990) leads only to minor changes in the resulting amplitudes and Fourier parameters.

Typical examples of synthetic UBVI-light curves are depicted in Fig. 2 for a fundamental mode pulsation and in Fig. 3 for a first overtone one, respectively. Further technical details will be presented in a forthcoming paper (Dorfi et al. 1999).

3. Results of radiative transfer calculations

3.1. Overall light curve structure

In Fig. 2 a typical example of synthetic UBVI light curves is plotted for a RR Lyrae model with stellar parameters corresponding to $M = 0.65\,\mathrm{M}_\odot$, $L = 52.5\,\mathrm{L}_\odot$, $T_{\rm eff} = 6600\,\mathrm{K}$ and $Z = 0.001$. The symbols refer to the different filters and the bolometric variation and all light curves are plotted with respect to their mean values $\langle m\rangle$ to reveal the amplitude differences. Since all further properties of the bolometric light curves (periods, amplitudes, Fourier coefficients) have been presented in Feuchtinger (1999b), we restrict the following discussion to the synthetic colour light curves.

It is evident that the differences between the bolometric light curve (plotted by the filled triangles) and the V light curve (plot-

Table 1. Pulsational properties of bolometric and UBVI-light curves for both model sequences. All models exhibit a luminosity of 52.5 $L_\odot$. Amplitudes (A) are given in magnitudes, $T_{\rm eff}$ denotes the effective temperature and P the pulsation period.

		Sequence A: M = 0.65 $M_\odot$, Z = 0.0010						Sequence B: M = 0.75 $M_\odot$, Z = 0.0001					
Mode	$T_{\rm eff}$ [K]	P [d]	$A_{\rm bol}$	A_U	A_B	A_V	A_I	P [d]	$A_{\rm bol}$	A_U	A_B	A_V	A_I
F	6000	0.849	0.188	0.299	0.277	0.209	0.129	-	-	-	-	-	-
F	6100	0.789	0.551	0.766	0.776	0.597	0.395	0.718	0.457	0.664	0.673	0.513	0.334
F	6200	0.741	0.769	1.007	1.079	0.826	0.520	0.673	0.715	0.933	0.996	0.768	0.491
F	6300	0.699	1.035	1.303	1.436	1.094	0.671	0.635	1.102	1.434	1.541	1.130	0.689
F	6400	0.660	1.109	1.383	1.524	1.160	0.708	0.600	1.231	1.645	1.763	1.301	0.757
F	6500	0.625	1.326	1.595	1.769	1.340	0.806	0.568	1.355	1.812	1.925	1.427	0.808
F	6600	0.592	1.390	1.666	1.837	1.391	0.836	0.539	1.491	1.934	2.053	1.523	0.874
F	6700	0.562	1.414	1.733	1.893	1.416	0.848	0.511	1.518	1.961	2.087	1.549	0.891
F	6800	0.534	1.369	1.709	1.864	1.389	0.819	0.486	1.227	1.554	1.735	1.278	0.741
F	6900	0.507	0.926	1.162	1.352	0.980	0.575	0.462	0.936	1.195	1.393	1.009	0.578
F	7000	0.483	0.593	0.742	0.869	0.640	0.363	0.440	0.739	0.940	1.106	0.811	0.465
1H	6800	0.398	0.430	0.541	0.622	0.460	0.264	0.364	0.519	0.684	0.770	0.576	0.335
1H	6900	0.379	0.396	0.497	0.571	0.422	0.241	0.347	0.495	0.636	0.725	0.540	0.311
1H	7000	0.361	0.356	0.436	0.501	0.369	0.209	0.331	0.463	0.577	0.657	0.490	0.280
1H	7100	0.344	0.338	0.427	0.491	0.362	0.203	0.316	0.400	0.499	0.569	0.425	0.241
1H	7200	0.329	0.247	0.308	0.355	0.263	0.144	0.302	0.309	0.381	0.439	0.327	0.183

ted by open pentagons) are very small yielding small bolometric corrections. The average difference between the V-band and the bolometric light curve (centered at their mean values) is given by 0.022 mag. As already known from observations (Lub 1977) and theoretical models (Bono et al. 1997) the amplitudes are largest in the B-band, followed by the U-, V- and I-bands for almost all effective temperatures. Further properties of the UBVI-light curves are summarized in Table 1. The relative changes in the shapes can be characterized by the variations of the corresponding Fourier coefficients which are discussed in Sect. 3.3.

Fig. 3 displays the theoretical UBVI-light curves together with the bolometric light curve around their mean values for a first overtone pulsator with $M = 0.65\,M_\odot$, $L = 52.5\,L_\odot$, $T_{\rm eff} = 6900\,{\rm K}$, $Z = 0.001$. Again, the V-band (plotted by open pentagons) follows closely the bolometric light curve (plotted by filled triangles) and the average deviation is 0.015 mag for this overtone model. The smallest amplitudes are found in the I-band and for all overtone pulsations we get an increasing sequence of amplitudes for the V-, U- and B-bands. Concerning both pulsational modes we see that the overall features like bumps at minimum light or knees in the descending part of the light curve are found in all calculated U-, B-, V- and I-bands. Furthermore we observe small shifts between the light curve maxima and minima of different passbands, which are of the order of a few percent of the period for both pulsational modes.

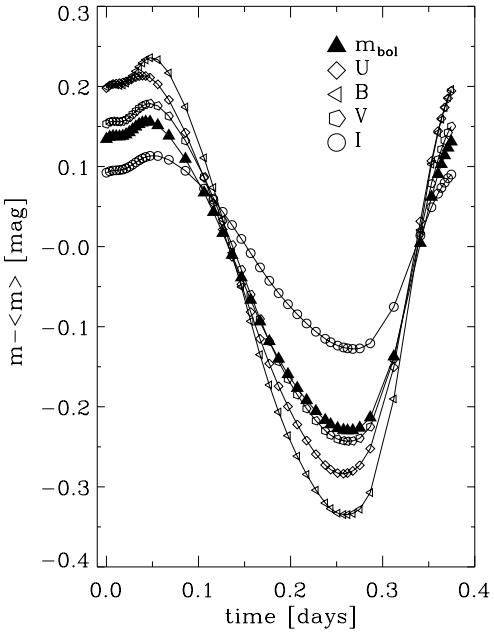

Fig. 3. Theoretical U-, B-, V-, I-band and bolometric light curves plotted around their mean values in each band for a first overtone RR Lyrae pulsation with $M = 0.65\,M_\odot$, $L = 52.5\,L_\odot$, $T_{\rm eff} = 6900\,{\rm K}$, $Z = 0.001$.

3.2. Pulsation amplitudes

Pulsation amplitudes for the different filters as well as bolometric amplitudes and pulsation periods are listed in Table 1. As already pointed out in Feuchtinger (1999b), the amplitudes depend on the parameters of the convection model and therefore do not result selfconsistently. The convective parameters (mixing length and turbulent viscosity) have been adjusted in order to obtain reasonable agreement of the bolometric amplitudes resulting from the nonlinear computations with the V amplitudes given in Simon & Teays (1982). The presented UBVI-light curves based on these calculations now put us in a position to perform a detailed comparison with observed pulsation amplitudes.

BVI amplitudes of globular cluster RR Lyrae stars are provided in Walker (1994, M68), Walker & Nemec (1996, IC4499) and Walker (1998, NGC 1851). While M68 is of metal-poor Oo

type II, IC4499 and NGC1851 belong to the intermediate-metal Oo type I. The comparison with our theoretical amplitudes is depicted in Fig. 5. For fundamental model pulsators it turns out that the maximum amplitudes exceed observed values for the B- and V-band, while I-band amplitudes agree reasonably with the maximum observed amplitudes. In general the fundamental mode amplitudes appear to be too large in order to fit the period-amplitude distributions for globular clusters. However, more models are necessary in order to investigate the origin of this disagreement. Most likely the convection parameters have to be adjusted more precisely, but also the particular choice of stellar parameters will influence the period-amplitude distribution. A much better agreement with observations is found for first overtone pulsators. Here for all three filters the amplitudes lie well within the observed sample. First overtone amplitudes appear to be less sensitive to changes in the free parameters of the convection model. Therefore an increase of the turbulent dissipation in order to adjust the fundamental mode amplitudes would not necessarily cause the first overtone amplitudes to be shifted out of the observed range.

I-band amplitudes for a large number of RR-Lyrae stars near the galactic center are provided by the OGLE project (Udalski et al. 1994). In order to estimate the corresponding B- and V-band amplitudes we use the following linear transformations derived from the above globular cluster data

$$A_{\rm V} = 0.075 + 1.497\,A_{\rm I} \qquad R^2 = 0.904 \qquad (1)$$
$$A_{\rm B} = 0.102 + 1.894\,A_{\rm I} \qquad R^2 = 0.886.$$

where a value of $R^2 = 1$ denotes perfect correlation whereas $R^2 = 0$ corresponds to the case of no correlation between the data. How the derived relations fit the observed data can be inferred from Fig. 4 where V-band and B-band amplitudes are plotted against I-band amplitudes for both RRab and RRc stars.

The comparison between OGLE amplitudes and theoretical amplitudes is plotted in Fig. 6. In general theoretical data fit better to the observations, even though for fundamental mode pulsations the B-band amplitudes also exceed the OGLE data. For V-band and I-band data the maximum amplitudes are located within the observational ranges. Analogous to the globular cluster case first overtone amplitudes fit better to the observed data.

From the theoretical UBVI amplitudes it is also possible to derive linear relations between bolometric and UBVI amplitudes. The coefficients of these relations are given in Table 2, and Fig. 7 shows the corresponding plots. Note that these transformations hold for both fundamental and first overtone pulsations

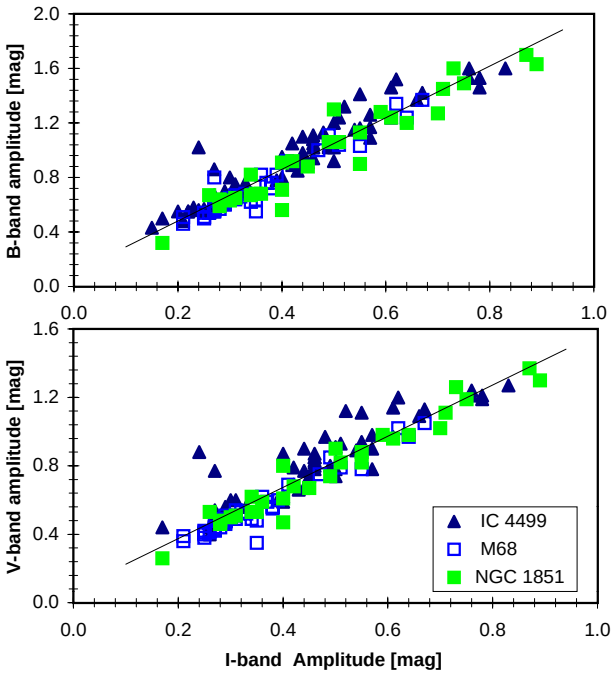

Fig. 4. B-band (upper panel) and V-band (lower panel) amplitudes as functions of I-band amplitudes for 3 globular clusters. Lines denote linear relations determined by a least square fit, observations are taken from from Walker 1994 (M68), Walker & Nemec 1996 (IC 4499) and Walker 1998 (NGC 1851).

Table 2. Transformation between bolometric and U-, B-, V- and I-band amplitudes (both fundamental and first overtone). R^2 denotes the quadratic correlation coefficient.

$A(X) = a + b\,A(Bol)$			
X	a	b	R^2
U	0.019	1.253	0.993
B	0.046	1.347	0.996
V	0.036	1.004	0.998
I	0.023	0.590	0.992

3.3. Fourier decomposition

3.3.1. Comparison with observed Fourier parameters

The comparison between theoretical and observed light curves by means of Fourier decomposition has been introduced by Simon & Lee (1981). Meanwhile due to several observational campaigns a large amount of observed Fourier parameters both for field and cluster RR Lyrae stars is available (e.g. Clement & Shelton 1997, Kovács & Kanbur 1997, Walker 1998, MSB98). However, due to the different photometric systems used in these investigations the data material is quite inhomogeneous. In this article we employ observed ranges of Fourier parameters up to the fifth order (field and cluster stars) provided by Kovács & Kanbur (1997) and recently published Fourier parameters of OGLE light curves near the galactic center (MSB98).

A comparison of the theoretical bolometric light curve parameters with the observed ranges given in Kovács & Kanbur (1997) has already been discussed in Feuchtinger (1999b). Observed data however, correspond to V-band light curves and consequently a comparison with bolometric parameters introduces some error. However, the differences between bolometric and V-band light curve parameters are negligible for amplitude ratios and remain below 10% for the phase differences. This can be seen from the linear relations between bolometric and V-band light curves derived from the theoretical models as discussed in

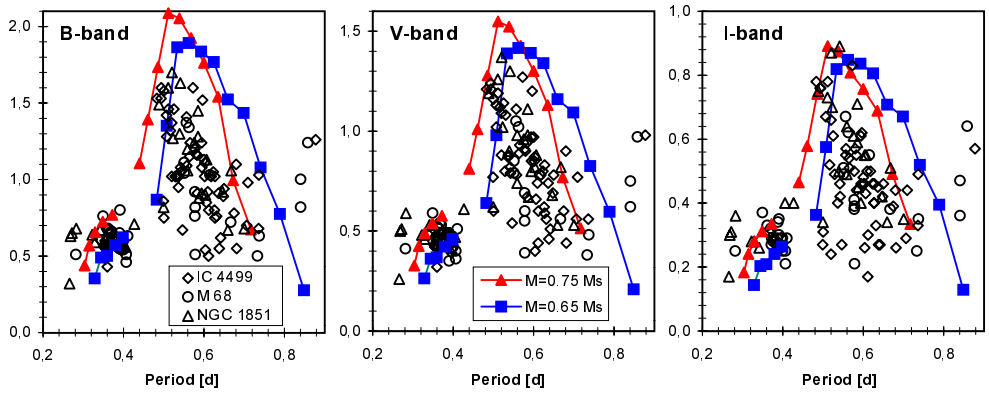

Fig. 5. Theoretical B-, V-, and I-band amplitudes as compared with observed globular cluster amplitudes from Walker 1994 (M68), Walker & Nemec 1996 (IC 4499) and Walker 1998 (NGC 1851).

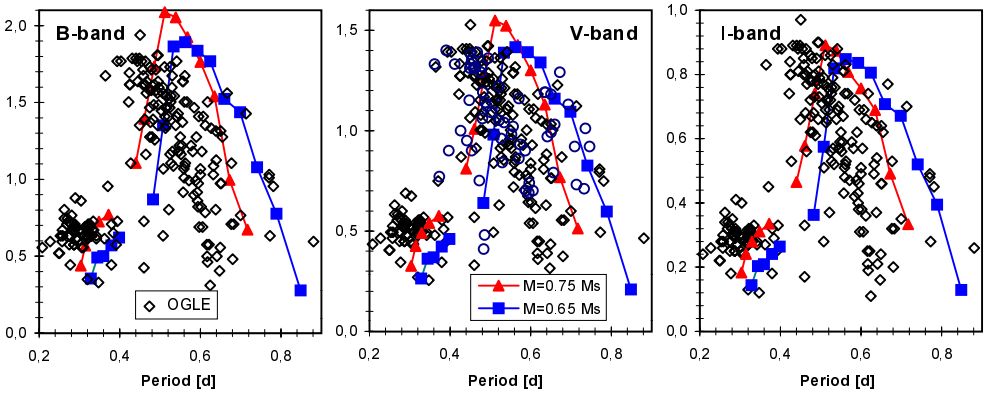

Fig. 6. Theoretical B-, V-, and I-band amplitudes as compared with observed OGLE amplitudes (Udalski et al. 1997). B- and V-band amplitudes are calculated from the I-band observations by applying the linear transformation laws given in Eq. 1. Open circles in the V-panel denote field star amplitudes taken from Simon & Teays (1982).

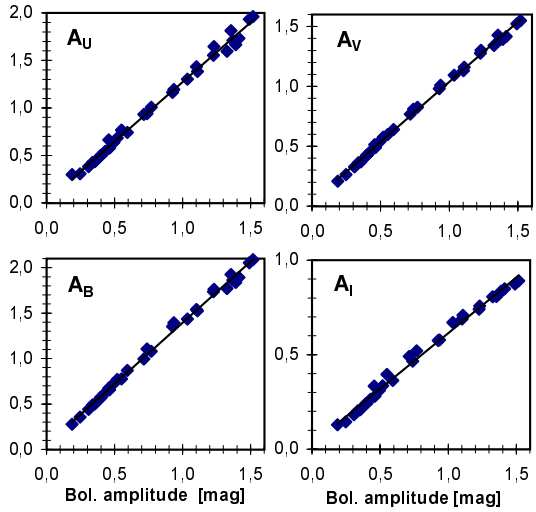

Fig. 7. Relations between bolometric and UBVI amplitudes. See text for details.

Sect. 3.3.2. Consequently, the general result already pointed out in Feuchtinger (1999b), that both amplitude ratios and phase differences are located within the observed V-band ranges, holds also for the presented theoretical V-band light curves.

OGLE light curves are observed in the near infrared I-band and here deviations between bolometric and I- band parameters are more pronounced, in particular for the phase differences. Using observed data from Walker (1994), who investigated BVI light curves from the M68 RR Lyrae population, MSB98 derived linear relations between V- and I-band Fourier parameters (cf. Sect. 3.3.3), which already have been used for a comparison in Feuchtinger (1999b). Here we can perform a direct comparison, which is depicted in Fig. 8 for RRab stars and in Fig. 9 for RRc stars. For the case of fundamental mode pulsations the Fourier amplitude ratios show good agreement up to the fifth order. The phase differences lie within the range of observations, even though they are systematically located at the lower boundary. However, theoretical results show the same trend of rising values with increasing pulsation period. Most likely the shift of the Fourier phases is a consequence of the particular choice of the free parameters (stellar parameters, turbulent convection), although a precice statment cannot be drawn on the basis of the two model sequences calculated so far.

First overtone pulsators show a similar agreement. Here both amplitude ratios and phase differences are located in the bulge of observed stars. It is interesting to note, that in contrast to RRab stars neither observations of RRc stars nor our theoretical models show a clear trend of the phase differences with period. In summary our theoretical results show reasonable agreement with observed OLGE data.

3.3.2. Bolometric-UBVI interrelations

Similar to the above mentioned linear relations between V-band and I-band Fourier parameters we derive linear relations between bolometric and UBVI-band parameters, but on a theoretical basis. For both pulsation modes these relations are compiled in Table 3. An impression of their fit quality can be estimated

Table 3. Coefficients of the linear transformations between U-, B-, V-, and I-band light curve Fourier parameters and bolometric ones. R^2 denotes the quadratic correlation coefficient.

U-Band: $X(U) = a + b\,X(Bol)$

$X(U)$	fundamental			first overtone		
	a	b	R^2	a	b	R^2
R_{21}	-0.012	0.998	0.985	0.005	1.018	0.976
R_{31}	-0.007	1.027	0.994	0.002	0.964	0.863
R_{41}	-0.011	1.108	0.967	0.006	0.745	0.777
R_{51}	-0.003	1.061	0.975	0.000	1.293	0.669
Φ_{21}	1.208	0.655	0.841	0.102	0.959	0.957
Φ_{31}	0.058	0.799	0.973	0.711	0.648	0.912
Φ_{41}	0.438	0.762	0.986	-1.221	1.672	0.664
Φ_{51}	0.628	0.720	0.967	1.117	0.750	0.769

V-Band: $X(V) = a + b\,X(Bol)$

$X(V)$	fundamental			first overtone		
	a	b	R^2	a	b	R^2
R_{21}	0.007	0.999	0.996	-0.011	1.058	0.980
R_{31}	-0.007	1.062	0.999	0.004	0.885	0.903
R_{41}	-0.002	1.068	0.996	0.008	0.805	0.756
R_{51}	-0.002	1.077	0.991	-0.001	1.590	0.729
Φ_{21}	0.518	0.861	0.984	-0.369	1.096	0.951
Φ_{31}	0.083	0.922	0.996	0.511	0.878	0.961
Φ_{41}	-0.065	0.879	0.994	0.525	0.519	0.544
Φ_{51}	0.502	0.863	0.981	0.042	1.012	0.913

B-Band: $X(B) = a + b\,X(Bol)$

$X(B)$	fundamental			first overtone		
	a	b	R^2	a	b	R^2
R_{21}	-0.004	0.943	0.995	-0.016	1.007	0.976
R_{31}	0.015	0.812	0.994	0.007	0.783	0.837
R_{41}	0.015	0.742	0.978	0.011	0.724	0.695
R_{51}	0.015	0.672	0.952	0.000	1.621	0.738
Φ_{21}	0.938	0.728	0.922	-0.981	1.231	0.914
Φ_{31}	0.055	0.837	0.989	0.471	0.849	0.947
Φ_{41}	-0.313	0.813	0.991	-0.833	1.672	0.752
Φ_{51}	0.462	0.795	0.979	0.343	0.945	0.884

I-Band: $X(I) = a + b\,X(Bol)$

$X(I)$	fundamental			first overtone		
	a	b	R^2	a	b	R^2
R_{21}	0.007	1.000	0.996	-0.011	1.058	0.980
R_{31}	-0.011	1.097	0.998	0.004	0.924	0.911
R_{41}	-0.002	1.098	0.992	0.008	0.823	0.786
R_{51}	-0.002	1.107	0.989	0.001	1.485	0.692
Φ_{21}	-0.571	1.209	0.988	-0.583	1.185	0.968
Φ_{31}	0.172	1.161	0.995	0.769	0.830	0.958
Φ_{41}	0.675	1.071	0.983	0.850	0.528	0.543
Φ_{51}	0.591	1.068	0.982	0.136	1.082	0.899

Table 4. Coefficients of the linear transformations between V-band and I-band light curve Fourier parameters and comparison to the transformations given in MSB98. R^2 denotes the quadratic correlation coefficient.

Fundamental mode: $X(V) = a + b\,X(I)$

$X(V)$	this paper			MSB98	
	a	b	R^2	a	b
R_{21}	-0.004	1.001	0.996	0.039	0.895
R_{31}	0.004	0.972	0.998	0.003	0.943
R_{41}	0.001	0.970	0.999	0.012	0.864
R_{51}	0.001	0.967	0.996	-	-
Φ_{21}	0.693	0.697	0.948	-0.376	1.010
Φ_{31}	-0.039	0.788	0.987	0.115	0.682
Φ_{41}	-0.611	0.810	0.986	-0.922	0.742
Φ_{51}	0.031	0.807	0.996	-	-

First overtone: $X(V) = a + b\,X(I)$

$X(V)$	this paper			MSB98	
	a	b	R^2	a	b
R_{21}	0.001	0.977	0.999	0.068	0.585
R_{31}	0.001	0.962	0.999	0.006	0.875
R_{41}	0.000	0.995	0.995	0.005	0.714
R_{51}	-0.001	1.037	0.990	-	-
Φ_{21}	0.144	0.930	0.994	1.929	0.555
Φ_{31}	-0.249	0.995	0.999	-0.512	1.059
Φ_{41}	-0.305	0.980	0.996	1.083	0.357
Φ_{51}	-0.101	0.938	0.999	-	-

by the quadratic correlation coefficient. In general fundamental mode parameters can be fitted with better quality than overtone models and amplitude ratios exhibit smaller R^2 values than phase differences. In particular the fits for some RRc phase differences show considerable scatter. However, the sample of overtone models is quite small, and more models are necessary in order to see if better defined relations can be found. In order to provide insight into the quality of the linear fits, as an example the low order Bol-V relations for both pulsation modes are plotted in Fig. 10.

3.3.3. V-I interrelations

The linear relations between V- and I-band Fourier parameters given in MSB98 can also be used for a comparison with our theoretical models. These relations are derived from observed V- and I-band light curves of the metal-poor galactic globular cluster M68 (Walker 1994). However, the number of stars used for setting up the relations is quite small (8 for RRab stars and 9 for RRc stars) and no correlation coefficients are given.

For fundamental mode pulsators this comparison is depicted in Fig. 11, while Table 4 provides the corresponding coefficients. As can be seen from the plots, the amplitude ratios show good agreement with the observed relations. In contrast larger deviations show up for some of the phase differences. In order to estimate the dependence on metallicity we provide extra plots for the two sequences, which differ by the amount of metallicity (Z = 0.001 for sequence A and Z = 0.0001 for sequence B). The maximum deviation occurs for the Φ_{21} values of sequence B. As the observed relations have been derived from metal-poor stars,

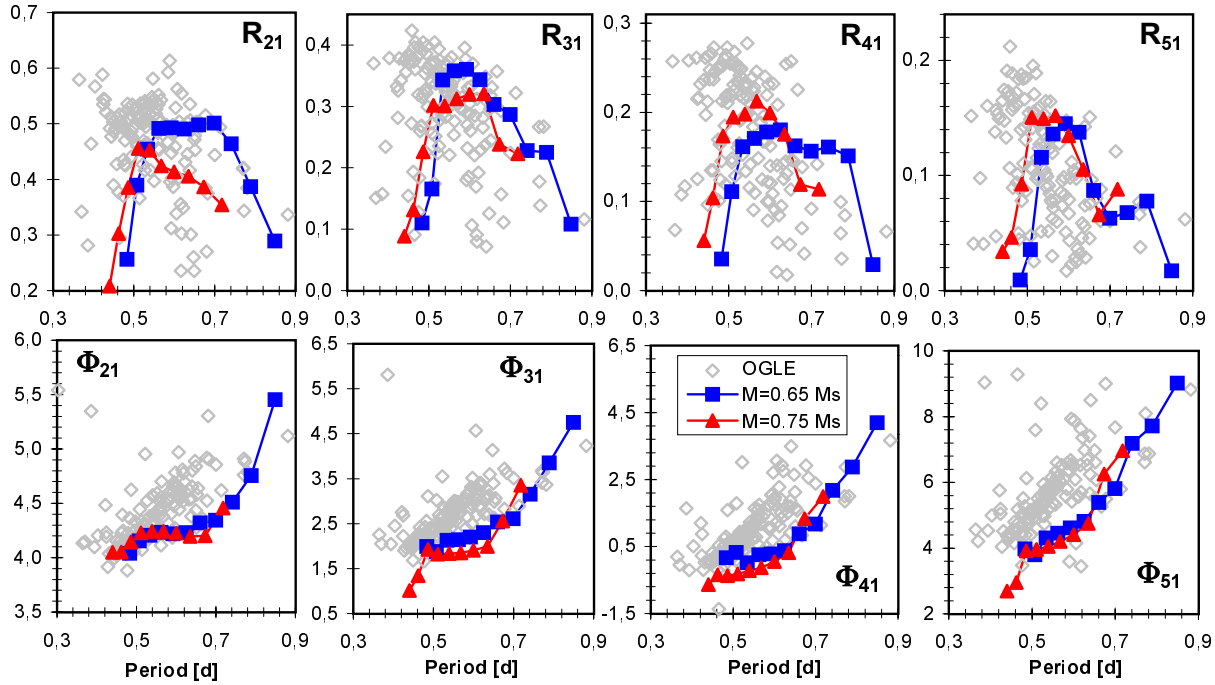

Fig. 8. Variation of the theoretical fundamental mode Fourier parameters of the I-band light curves with respect to the pulsation period. The gray diamonds denote OGLE data according to MSB98.

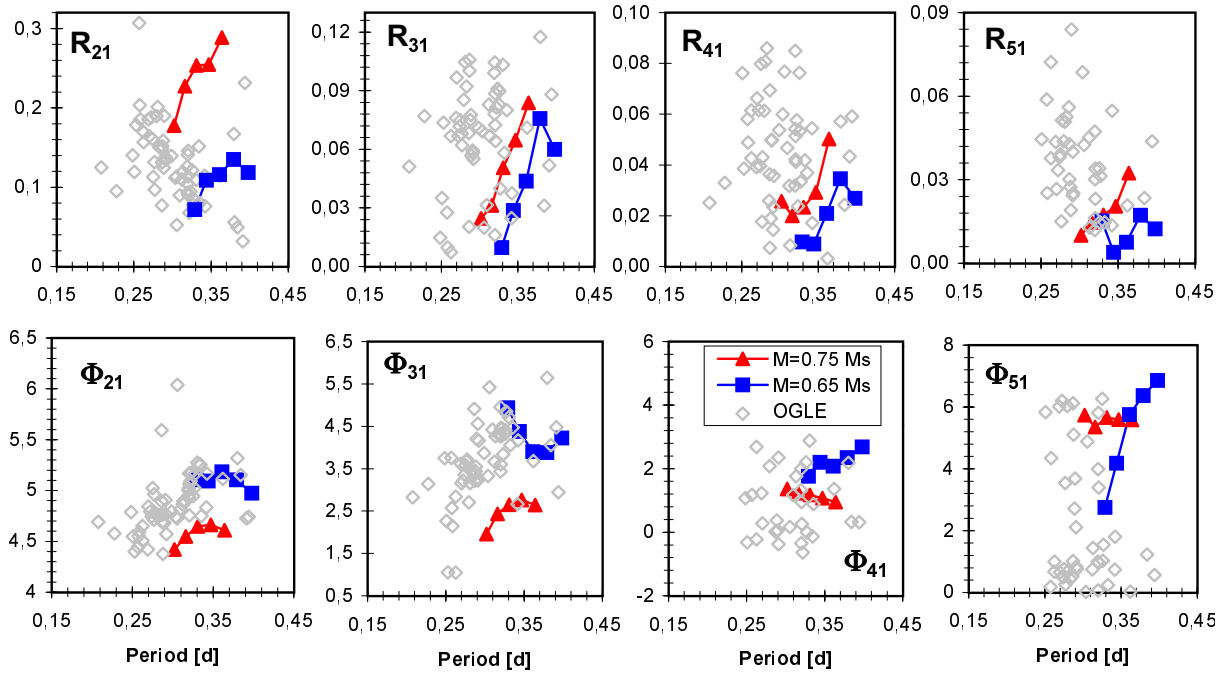

Fig. 9. Variation of the theoretical first overtone mode Fourier parameters of the I-band light curves with respect to the pulsation period. The gray diamonds denote OGLE data according to MSB98.

one would expect, that sequence B should exhibit better agreement. However, for the case of Φ_{21} the opposite holds. For Φ_{31} sequence B shows better agreement, while there is almost no difference for Φ_{41}. Consequently no distinct metallicity effect can be followed from these results. In fact much more models covering a wider range of stellar parameters are needed in order to investigate the systematics of such deviations.

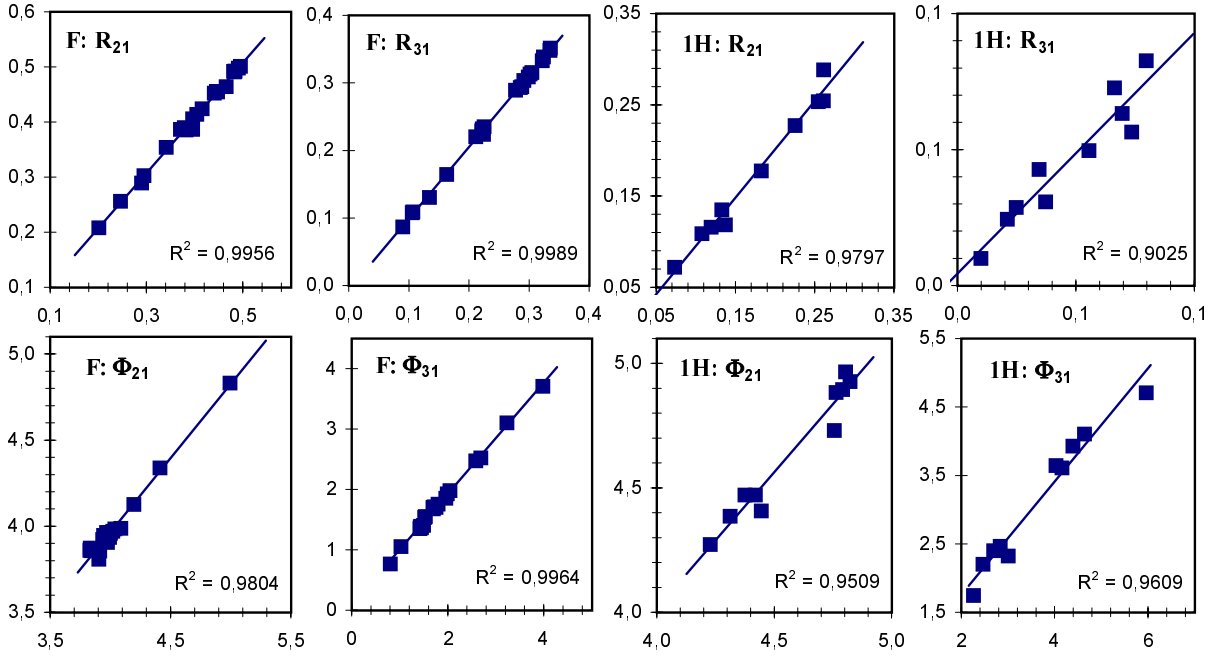

Fig. 10. Transformations between theoretical bolometric (x-axis) and theoretical V-band (y-axis) low order Fourier parameters. F denotes fundamental and 1H first overtone pulsations, R^2 the quadratic correlation coefficient.

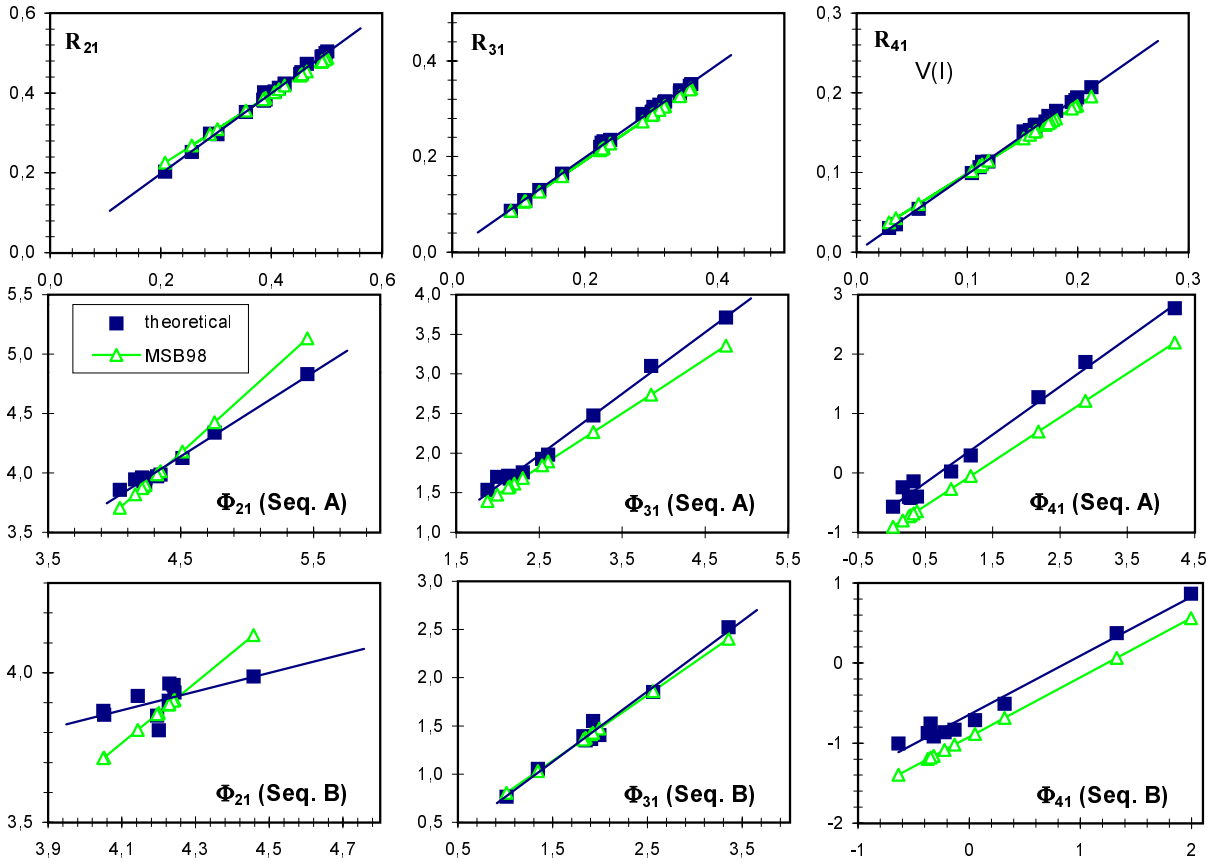

Fig. 11. Theoretical relation between V-band and I-band Fourier parameters in comparison with observed relations given in MSB98. The x-axes correspond to I-band values, y-axes to V-band values. In order to show the effect of different metallicities, the phase differences for the two model sequences are plotted separately.

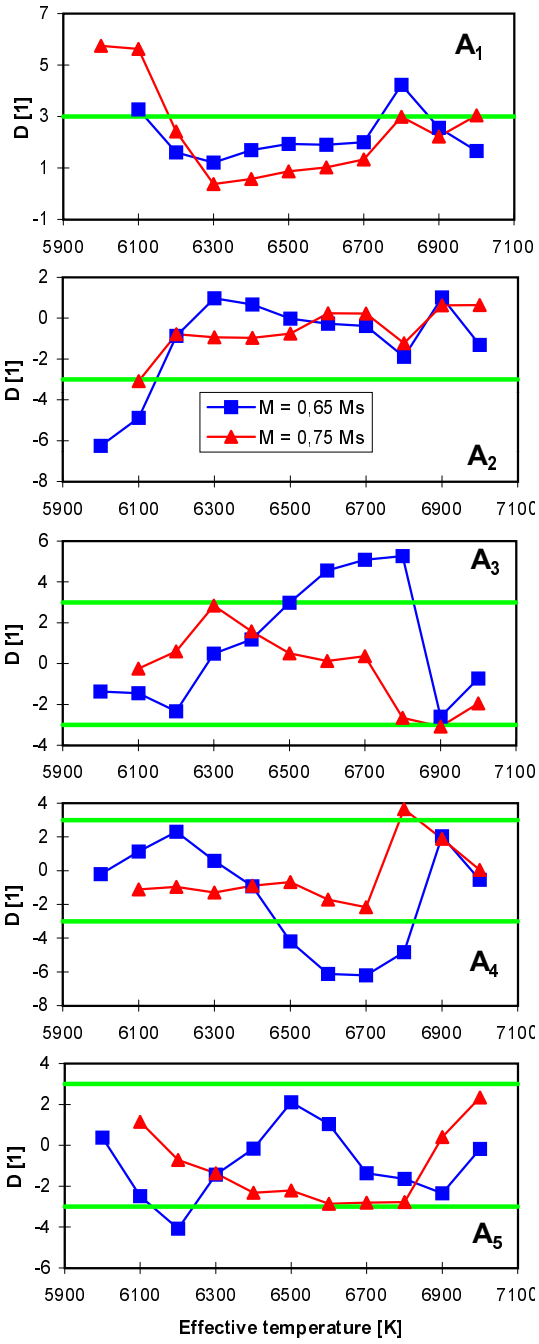

Fig. 12. Comparison with the morphological interrelations given in Kovács & Kanbur (1997): Normalized differencees between theoretical Fourier amplitudes and the values predicted by the interrelations for the fundamental mode light curves. The horizontal lines denote the range of compatibility. See text for details.

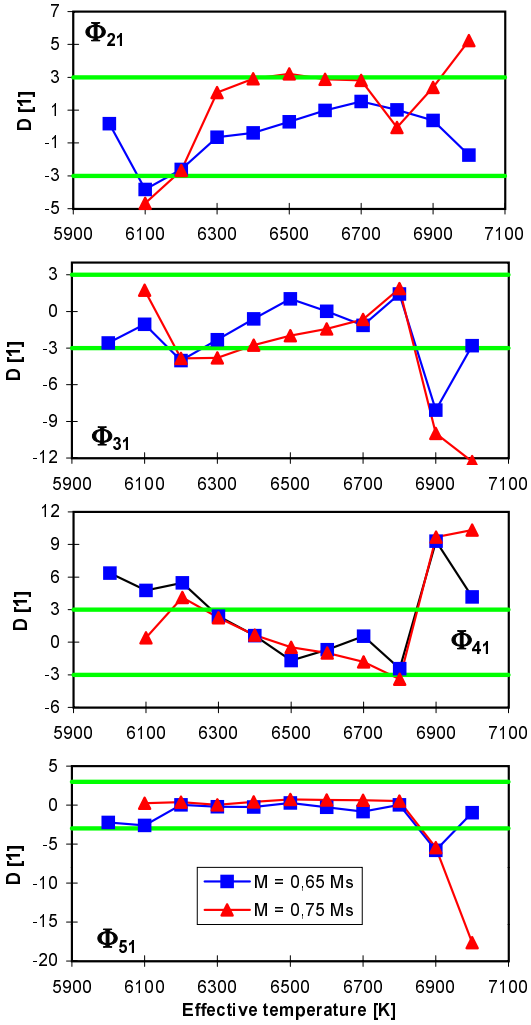

Fig. 13. Comparison with the morphological interrelations given in Kovács & Kanbur (1997): Normalized differences between the theoretical phase differences and the values predicted by the interrelations for the fundamental mode light curves. The horizontal lines denote the range of compatibility. See text for details.

3.3.4. Empirical relations

In Kovács and Kanbur (1997) empirical relations between observed Fourier parameters of both field and cluster RRab stars have been derived. A comparison with our bolometric light curves using these relations has already been presented in Feuchtinger (1999b), where a detailed discussion can be found. Here we use the computed V-band light curves instead of the bolometric ones. For the Fourier amplitudes the results are plotted in Fig. 12, while the phase differences are depicted in Fig. 13. We plot the normalized differences given in Kovács and Kanbur (1997, Eq. 4), where for compatibility with observations a range of $\pm 3\sigma$ is demanded. This range is denoted by the shaded horizontal lines. As main result from this comparison it turns out, that in particular for the low order parameters our models show good compatibility with the empirical relations. For the higher orders some deviations occur, even though remarkable agreement is e.g. found for Φ_{51}. As expected, V-band light curves show smaller deviations from the empirical relations than the bolometric ones. An interesting effect concerns Φ_{21}, where the majority of the V-band light curves of sequence B lie within the compatibility range, while the bolometric ones are located outside (Fig. 10 in Feuchtinger 1999b). This emphasizes the

importance of detailed radiative transfer calculations, if such detailed comparisons with observations are performed.

4. Conclusions

The presented radiative transfer calculations allow a direct comparison of the observed RR Lyrae light curves in different photometric passbands with the our theoretical pulsation models. We have used recent data on globular clusters from Walker (1994, 1998) and Walker & Nemec (1996) as well as OGLE data (Udalski et al. 1994,1997, MSB98) and find good agreement with observed amplitudes and Fourier parameters in the corresponding filter bands. The theoretical models are located more on the upper boundary of the amplitudes for fundamental mode pulsations but agree perfectly for the first overtone pulsations. Since up to now we have compared and computed only two model sequences and since the amplitudes depend on the parameter of the adopted model of turbulent energy transport (see Feuchtinger 1999ab for the details) we think that this small difference can be resolved by further computations with more carefully adjusted parameters.

From comparing theoretical UBVI light curves with the bolometric ones we have computed linear relations to transform pulsation amplitudes and Fourier parameters from one band into the others. Some of these relations can directly be compared with relations derived from observations (MSB98) yielding reasonable agreement. Even though these relations are based on only two model sequences, they exhibit good correlations and can be used to estimate UBVI properties from bolometric ones.

Summarizing the effects of the radiative transfer calculations on the Fourier decomposition results, we found that in comparison with bolometric light curves (Feuchtinger 1999b) the overall agreement between theory and observation become even better. In particular the morphological relations found by Kovács & Kanbur (1997) can be reproduced at least for the low order Fourier parameters.

In summary by introducing the frequency dependence of the emerging radiation field for the analysis of theoretical RR Lyrae light curves, we can reproduce the main features of observed RR Lyrae curves for fundamental as well as for first overtone pulsators.

Acknowledgements. We are greatly indebted to Dr. F. Kupka for providing us with frequency dependent Kurucz opacities. This work is supported by the *Fonds zur Förderung der wissenschaftlichen Forschung (FWF)* under project number S7305–AST.

References

Alcock C., Allsman R.A., Alves D.R., et al., 1998, ApJ 492, 190
Alexander D.R., Augason G.C., Johnson H.R., 1989, ApJ 345, 1014
Balluch M., 1988, A&A 200, 58
Bessell M.S, 1990, PASP 102, 1181
Bono G., Caputo F., Castellani V., Marconi M., 1997, A&AS 121, 327
Bono G., Stellingwerf R.F., 1994, ApJS 93, 233
Clement C.M., Shelton I., 1997, AJ 113, 1711
Dorfi E.A., Feuchtinger M.U., Kupka F., 1999, in prep.
Feuchtinger M.U., 1998, A&A 337, L29
Feuchtinger M.U., 1999a, A&AS 136, 217
Feuchtinger M.U., 1999b, A&A, subm.
Feuchtinger M.U., Dorfi E.A., 1994, A&A 291, 225
Feuchtinger M.U., Dorfi E.A., 1998, In: A half century of stellar pulsation interpretations: A tribute to Arthur N. Cox. PASPC 135, 297
Iglesias C.A., Rogers F.J., 1991, ApJ 371, 408
Kolláth Z., Beaulieu J.P., Buchler J.R., Yecko P., 1998, ApJ 502, L55
Kovács G., Kanbur S., 1997, MNRAS 295, 834
Kurucz R.L., 1993, CDROM 13: ATLAS9.SAO, Harvard, Cambridge
Landolt-Börnstein, 1982, Numerical Data and Functional Relationships in Science and Technology, Astronomy & Astrophysics. Vol. 2, Springer, Berlin, p. 35ff
Lub J., 1977, A&AS 29, 345
Morgan S.M., Simet M., Bargenquast S., 1998 (MSB98), Acta Astron. 48, 341
Simon N.R., Kanbur S., 1993, ApJ 451, 703
Simon N.R., Lee A.S. 1981, ApJ 248, 291
Simon N.R., Teays T.J., 1982, ApJ 261, 586
Späth H., 1983, Spline-Algorithmen. Oldenbourg, Wien
Udalski A., Kubiak M., Szymonski M., et al., 1994, Acta Astron. 44, 317
Udalski A., Olech A., Szymonski M., et al., 1997, AcA 47, 1
Walker A., 1994, AJ 108, 555
Walker A., 1998, AJ 116, 1005
Walker A., Nemec J.M., 1996, AJ 112, 2026
Wuchterl G., Feuchtinger M.U., 1998, A&A 340, 419
Yorke H.W., 1980, A&A 86, 286